

# Formation of a coupled state in a laser plume

N.E. Kask, S.V. Michurin, G.M. Fedorov, D.B. Choporniyak

**Abstract.** The results of experimental investigation of a low-temperature plasma produced by laser irradiation at the surface of metal targets are reported. The optical characteristics and the plasma pressure in the laser plume are found to exhibit a threshold behaviour under vaporised-material density variation. The results are interpreted using the model of a coupled plasma state with limitation of plasma expansion.

**Keywords:** laser plume, coupled plasma, fractal structures, radiation–substance interaction.

## 1. Introduction

In the last decades, the interest in the study of the physical properties of small metallic particles randomly distributed in a dielectric matrix is due to the discovery of giant enhancement of nonlinear-optical phenomena near the surface of small particles [1–3], on the one hand, and the development of new nanoparticle production techniques, in particular, the pulsed laser ablation technique, on the other hand [4, 5]. Laser evaporation is accompanied by the production of a low-temperature cluster plasma in which nanoparticles (clusters) are formed. A cluster plasma is an efficient light source with a continuous spectrum, which is well approximated by the blackbody radiation spectrum with a colour temperature significantly higher than for incandescent lamps. Compact clusters may coagulate to form branched fractal structures.

It was earlier found out [6] that efficient fractal formation takes place during a 10-ms laser pulse. Fractals, both in micro- and macroscopic forms, are efficiently produced as a result of the following sequence of processes:

- (i) vapour condensation with the production of compact nanoparticles (droplets, clusters);
- (ii) ejection of the nanoparticles by the thermophoretic force to the periphery of the laser plume;

(iii) deceleration of the nanoparticles by the Stokes force and their accumulation in some layer surrounding the plume plasma;

(iv) aggregation of the nanoparticles into either weakly coupled fractal microclusters or a macroscopic fractal structure (shell) with a rather strong coupling capable of limiting the plasma expansion.

Microcluster formation is observed at relatively low plasma densities realised in the erosion plume regime. In order for a fractal shell to emerge, the critical particle number density should be exceeded; above this density there occurs a limitation of plasma expansion and a decrease in the dimensions of the plasma region, and a sharp boundary of this region is formed [6, 7]. All this is more in the nature of a drop rather than a gas plume; by analogy with Ref. [8], this state will be referred to as a coupled state.

Condensation and coupled-state formation in a plasma should affect the rate of pressure change in the gas–vapour region in passing through the corresponding critical particle number density of the vaporised material. While the formation of a condensate (compact nanoparticles) always takes place upon laser target ablation into the ambient gas, the formation of a coupled plasma state is characterised by a clearly defined threshold pressure. In this work, we studied laser radiation absorption in the plume, both in the erosion regime of target evaporation and in the coupled-plasma regime, with the aim of establishing the correlation between this absorption and the variation in pressure inside the chamber during the laser pulse.

## 2. Experimental

A pulsed solid-state neodymium-glass laser was employed for irradiation [9]. The 1.06-μm, 100-J nonpolarised radiation was bell-shaped and had the FWHM  $\tau_{1/2} \approx 10$  ms.

The target vaporised by the laser radiation was accommodated in a leakproof chamber – a steel hollow cylinder with quartz windows and the internal cavity measuring 25 mm in diameter and 150 mm in length. As a buffer gas determining the external pressure, we used 99.99 % pure He, Ar, and Kr. The pressure in the chamber could be varied between 0.001 and 100 atm.

The targets were polycrystalline metallic samples with a purity of 99.9 % and higher, whose irradiated surface underwent grinding. Check experiments with samples subjected to surface finish of different degree (grinding, polishing) as well as with repeated irradiation allowed a conclusion that the quality of surface processing does not play any significant role in the irradiation duration range

N.E. Kask, S.V. Michurin, G.M. Fedorov, D.B. Choporniyak  
D.V. Skobeltsyn Institute of Nuclear Physics, M.V. Lomonosov Moscow State University, Vorob'evy gory, 119992 Moscow, Russia;  
e-mail: nek@srn.sinp.msu.ru

under investigation. The typical dimensions of samples were  $1 \times 1 \times 0.5$  cm.

The laser radiation propagating along the axis of experimental chamber was focused with a spherical lens with a focal distance  $F_1 = 300$  mm into a spot of diameter  $d \approx 2$  mm on the target surface.

The pressure variation ( $\Delta P$ ) inside the chamber during and after laser irradiation was recorded with a piezoelectric sensor operating in the regime of a voltage generator with an  $RC$  constant  $\tau_{RC} \sim 5$  ms. The sensor had a diameter of  $\sim 10$  mm and a thickness of 1 mm. The sensor was shielded with a metal foil to avoid photoinduced pickup from the heating laser radiation.

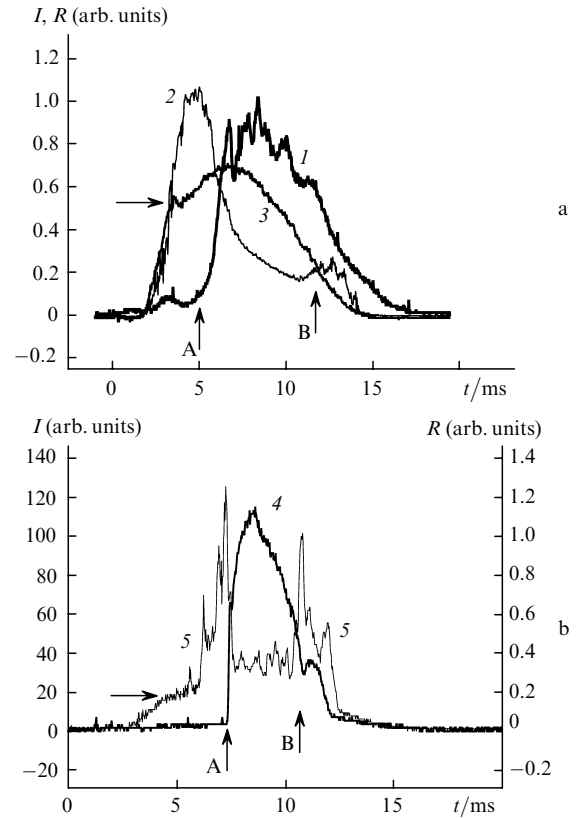
### 3. Laser radiation absorption by the plume plasma and morphology of damage

The kinetics of plume glow and of the laser radiation absorbed and scattered from the target surface were studied by using photoelectronic radiation recording. As a rule, analysis of the signals permits determining the instant of melt production [10] and the onset of boiling or the appearance of breakdown plasma. In our experiments, when an unpolished surface was irradiated, its melting brought about an increase in the reflection signal, which subsequently became appreciably weaker upon the emergence of a gas-vapour phase (boiling). For relatively small laser radiation fluxes, the growth of the glow intensity became slower for some time when the surface temperature reached the melting point during heating. The plasma emerging in the vapour masks the liquid-vapour phase transition, and the glow signal kinetics reflects the growth of plasma region dimensions and plasma temperature instead of stabilisation of the surface temperature at the moment the boiling point is reached.

Figure 1 shows typical oscilloscope traces. The signals (Fig. 1a) were recorded at a pressure of 1 atm, which corresponds to the case of erosion plasma, when there occurs no aggregation of fractal structures into a macroscopic shell. At the same time, in the plasma volume there already exist microregions with enhanced absorptivity, which manifests itself in a decrease of backscattered laser-radiation signal [curve (2)] and an appreciable increase in the glow signal. When the pressure exceeds the threshold for the formation of a macroscopic shell (Fig. 1b), the glow intensity of plasma in the coupled state increases further by two orders of magnitude [curve (4)].

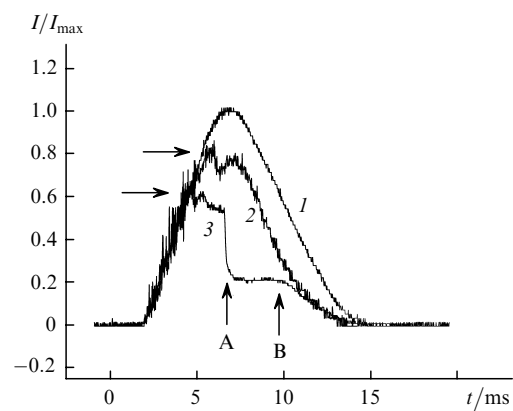
To estimate the energy absorption in the plasma plume, we studied the attenuation dynamics of the laser radiation transmitted through the plume. Usually [11], a small opening in the sample located at the centre of the heating spot is employed for such measurements. In the case of a millisecond laser pulse, an opening with a diameter of about 0.5 mm is repeatedly closed even in a thin metal foil ( $\sim 0.5$  mm) during irradiation. This is the reason why in our work the radiation was focused either on the edge of a sample or on the transverse foil section located along of the laser caustic. As a calibration signal, we used a laser pulse with an intensity below the threshold for target material vaporisation.

Figure 2 shows typical oscilloscope traces of the radiation intensity transmitted through the plume plasma (at the surface of an aluminium target in this case) for two values of external pressure: below and above the threshold of coupled



**Figure 1.** Oscilloscope traces of plasma plume glow  $I$  (1, 4) and of Nd laser radiation  $R$  scattered in the backward (2, 5) and transverse (3) direction for buffer gas pressures  $P = 1$  (a) and 10 atm (the coupled plasma regime) (b) in the case of nickel target irradiation. Horizontal arrows indicate the instants of appearance of erosion plasma, vertical arrows indicate the instants of coupled-plasma microregions formation (A) and the onset of their decay (B).

plasma production. In the general case, the attenuation of transmitted radiation is characterised by the extinction coefficient, which includes, apart from radiation absorption, light scattering in the medium as well. The latter may be



**Figure 2.** Oscilloscope traces of transmission signals for incident laser radiation for the plasma at the surface of an aluminium target: the laser pulse shape (1), the plasma transmission signal for buffer gas pressures  $P = 1$  (2) and 30 atm (3). Horizontal arrows indicate the instants of appearance of erosion plasma, vertical arrows indicate the instants of coupled-plasma microregions formation (A) and the onset of their decay (B).

neglected under our experimental conditions, because the emergence of the plasma plume is not accompanied by a growth in the scattered radiation intensity (see Fig. 1). As follows from Fig. 2, the plume absorptivity in the erosion plume regime is significantly lower than in the coupled plasma regime, where it approaches unity.

The emergence of plasma and the absorption of laser radiation in the laser plume result in a pressure rise in the chamber. It would appear natural that the pressure jump would increase with increasing absorption. The dependences of the jump  $\Delta P$  and the efficiency of fractal formation [6] on the initial pressure of the buffer gas are presented in Fig. 3. In the erosion plume regime, which takes place at below-threshold pressures,  $\Delta P$  is observed to grow steadily with  $P$ . Near the threshold,  $\Delta P$  decreases almost simultaneously with the lowering of fractal formation efficiency. The above-threshold plasma, as our measurements suggest (see Fig. 2), possesses a higher absorptivity, and it is evident that the decrease of  $\Delta P$  is a consequence of the formation of a coupled state.

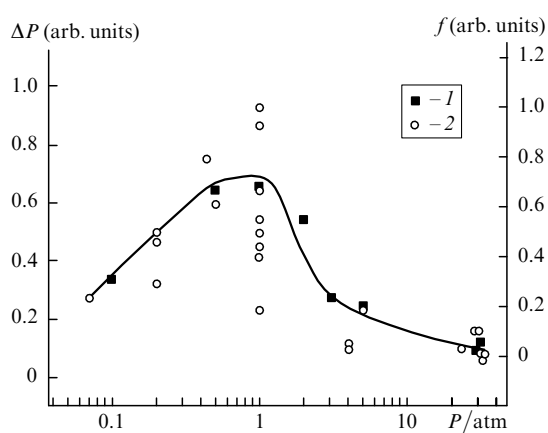


Figure 3. Fractal formation efficiency  $f$  (1) and pressure step  $\Delta P$  (2) as functions of pressure in the irradiation of a vanadium target.

The minimal longitudinal dimension of the plasma region, prior to the moment the absorption wave detaches from the surface, is comparable to the transverse dimension of the focal waist of laser radiation caustic. The depth of laser radiation penetration into such plasma does not exceed several tenths of a millimetre. The plasma screens the surface from the incident radiation but at the same time it cannot help transferring the thermal energy to the surface. In the one-dimensional approximation, the heating depth  $h$  during the laser pulse is determined by thermal diffusion and by the order of magnitude  $(4\chi\tau)^{1/2}$ , where  $\chi$  is the thermal diffusivity and  $\tau$  is the laser pulse duration. Since the surface temperature in both regimes is equal to the metal boiling temperature, the depths of heating, for instance to the metal melting temperature, also prove to be the same towards the end of the laser pulse ( $h \sim 1$  mm). Therefore, the thermal energy losses due to the contact between the plasma and the target do not change significantly in going from the erosion plasma regime to the coupled plasma regime.

Furthermore, the crater in the coupled plasma regime is significantly smaller in depth ( $\sim 100$   $\mu$ m), quite often with a cone protruding at the centre whose volume exceeds the volume of the metal expelled and the height amounting to  $\sim 2$  mm. In some cases (Pb, Re), a solidified figure of length

above three millimetres is observed which can be approximated by a cylinder and is directed towards the laser radiation. The location of these objects at the crater centre contradicts to the commonly accepted model of melt extrusion [12], and it may be assumed that they emerge after cooling of the strongly coupled plasma object with a high surface tension. One can see from the photograph of a cone section that the cone is filled with a porous (foamed) metal (Fig. 4). Upon the vapour cooling, the plasma passes into an 'expanded' metal liquid, which remains coupled to the melt at the sample surface due to the surface tension forces.

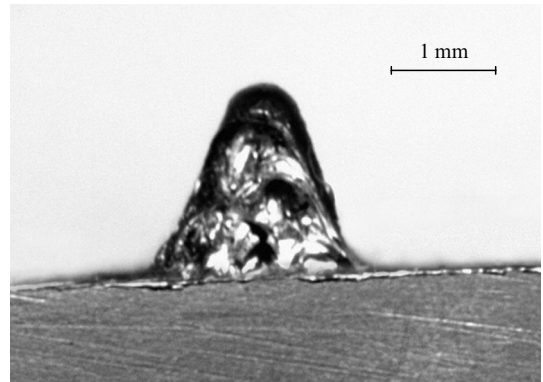


Figure 4. Photograph of the section of a cone appearing on the irradiated nickel surface;  $P = 10$  atm.

As found out in Ref. [6], fine-dispersed particles are accumulated in sufficiently hot layers at the plume periphery, to form a fractal shell under certain conditions. At pressures close to the threshold value for plasma transition to the coupled state, the shell, after flying off the plume, is observed as a fractal macrostructure after cooling [6]. Obviously, the situation is also possible when the shell, which confines the plasma in the coupled state, is rather strongly connected to the sample and contracts under the action of the surface tension forces and solidifies during cooling to form fused structures. The continuing plasma degradation inside the closed volume of these objects leads to the formation of cavities.

At lower pressures, in the erosion plume regime, a vaporised material jet is produced. Under certain conditions – for a sufficiently large recoil momentum of the vapour jet – the melt is forced out of the crater and a droplet fraction appears at its boundaries and in the plume. For several metals we observed even deeper craters (about several millimetres in depth) and an abundant ejection of melt when the external pressure was brought down below some critical level dependent on the group number in the Mendeleev Periodic Table. In particular, in rare-earth element samples, the craters with a diameter  $d \sim 2$  mm and a depth  $\delta \sim 4$  mm were produced when the buffer gas pressure  $P$  did not exceed 0.1 atm. The following values are typical for metals of the first (Li, Na) and fourth (Ti, Zr, Hf) groups of the Periodic Table:  $d \sim 2$  mm,  $\delta \sim 3$  mm, and  $P \leq 1$  atm. Similarly, for elements of the second group (Zn, Cd), we have  $d \sim 0.5$  mm,  $\delta \sim 3$  mm, and  $P \leq 20$  atm. It is commonly assumed [12] that deep ('dagger-shaped') damage by single pulses takes place due to the increase in the heating radiation intensity near the bottom of the cavern due to

radiation reflection from its walls and the reduction of bottom area. A nonlinear process is missing from this model to account for the threshold dependence on the external pressure observed in our work. This threshold effect is the formation of a coupled plasma state. Inside the cavern, the threshold of this process is significantly lowered due to the limitation of vapour expansion in the transverse direction. The plasma in the coupled state possesses a higher absorptivity, which provides an increase in the inflow of thermal energy to the cavern walls compared to the erosion regime. The low external pressure does not prevent the ejection of plasma and melt material from the cavern.

#### 4. Conclusions

It is known that as the density of a condensed disperse phase introduced into a low-temperature plasma the interaction between condensate particles may become stronger to the extent that the gas plasma transforms into a plasma drop [8]. A similar situation also occurs in the case of a laser plasma produced upon target evaporation by millisecond laser pulses in the buffer gas atmosphere. A macroscopic fractal shell forms in the peripheral layers of the plasma region when the external pressure produced by the buffer gas exceeds some critical value determined by the target material. In this case, several plasma characteristics experience a stepwise change, which is manifested in the characteristic emission kinetics and in absorption and scattering of laser radiation in the plume volume. The expansion of the vaporised material is substantially limited, the plasma liquid gradually transforms upon cooling to an expanded metal and a porous melt, which are coupled to the target by the surface tension force, and therefore a pressure jump in the ambient gas is absent.

**Acknowledgements.** This work was supported by the Russian Foundation for Basic Research (Grant Nos 03-02-17026 and NSh-1771.2003.2)

#### References

1. Emel'yanov V.I., Koroteev N.I. *Usp. Fiz. Nauk*, **135**, 345 (1981).
- doi> 2. Moskovits M. *Rev. Mod. Phys.*, **57**, 783 (1985).
3. Antsiferov V.V., Smirnov G.I., Telegin G.G. *Opt. Spektrosk.*, **79**, 487 (1995).
- doi> 4. Smirnov B.M. *Usp. Fiz. Nauk*, **170**, 495 (2000).
- doi> 5. Anisimov S.I., Luk'yanchuk B.S. *Usp. Fiz. Nauk*, **172**, 301 (2002).
- doi> 6. Kask N.E., Leksin E.G., Michurin S.V., et al. *Kvantovaya Elektron.*, **32**, 437 (2002) [*Quantum Electron.*, **32**, 437 (2002)].
- doi> 7. Kask N.E., Michurin S.V., Fedorov G.M. *Kvantovaya Elektron.*, **33**, 57 (2003) [*Quantum Electron.*, **33**, 57 (2003)].
8. Samsonov D., Goree J. *Phys. Rev. E*, **59**, 1047 (1999).
- doi> 9. Kask N.E., Fedorov G.M. *Kvantovaya Elektron.*, **23**, 1033 (1996) [*Quantum Electron.*, **26**, 1007 (1996)].
- doi> 10. Banishev A.F., Golubev V.S., Dubrov V.D. *Kvantovaya Elektron.*, **23**, 1029 (1996) [*Quantum Electron.*, **26**, 1003 (1996)].
11. Bulgakova N.M., Bulgakov A.V. *Appl. Phys. A*, **73**, 199 (2001).
12. Vedenov A.A., Gladush G.G. *Fizicheskie protsessy pri lazernoi obrabotke materialov* (Physical Processes in Laser Material Processing) (Moscow: Energoatomizdat, 1985).